Heliyon 11 (2025) e42503

Contents lists available at ScienceDirect

Heliyon

journal homepage: www.cell.com/heliyon

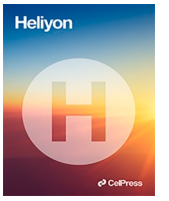

Research article

Reverse transcription-quantitative PCR assays for detecting SARS-CoV-2 using subgenomic RNA load

Yun-Hsiang Cheng [a,c], Cheng-Hsiu Chen [a,b], Ping-Cheng Liu [a,d], Wen-Ting Chen [a], Chi-Ju Hsu [a,b], Cheng-Cheung Chen [a,b,c], Jun-Ren Sun [a,b,c,e,*]

[a] *Institute of Preventive Medicine, National Defense Medical Center, Taipei, Taiwan*
[b] *Graduate Institute of Medical Science, National Defense Medical Center, Taipei, Taiwan*
[c] *Graduate Institute of Biodefense, National Defense Medical Center, Taipei, Taiwan*
[d] *Graduate Institute of Applied Science and Technology, National Taiwan University of Science and Technology, Taipei, Taiwan*
[e] *Division of Infectious Diseases and Tropical Medicine, Department of Internal Medicine, Tri-Service General Hospital, National Defense Medical Center, Taipei, Taiwan*

A R T I C L E I N F O

Keywords:
SARS-CoV-2
Rodent model
Gene copy number
Plaque assay
Subgenomic RNA

A B S T R A C T

SARS-CoV-2, the virus responsible for COVID-19, triggers the synthesis of full-length genomic RNA (gRNA) and subgenomic RNAs (sgRNAs) in host cells upon infection. Traditional PCR aimed at targeting gRNA to detect viral presence is insufficient. sgRNAs serve as novel markers for active viral replication. However, the utility of reverse transcription-quantitative PCR (RT-qPCR) assays targeting sgRNAs as indicators of active viral load and infectivity in rodent models has not been validated. We developed four RT-qPCR assays targeting the SARS-CoV-2 genes—ORF1ab, N, E, and E-sgRNA and two RT-qPCR assays for housekeeping genes Hamster *Gapdh*, and Mouse *Actb*. We used serial dilutions to establish standard curves for quantification. These assays demonstrated high amplification efficiency (96%–97 %) and a strong correlation between the cycle threshold (Ct) values and logarithmic copy number of the genes ($R^2 = 0.9933–0.9996$). Analyzing 102 residual rodent lung tissue samples, we compared the viral loads quantified using RT-qPCR assays with those determined by viral culture. A strong correlation emerged between the RT-qPCR assays' detection of positivity and the viral culture results. Notably, the quantification of viral loads using the E-sgRNA RT-qPCR assay correlated more closely with viral culture outcomes than with other targets ($r = 0.93$, $p < 0.001$). These results underscore the sgRNA RT-qPCR assay's potential for tracking actively replicating viruses in rodent models infected with SARS-CoV-2, offering a reliable alternative to traditional viral culture methods.

1. Introduction

Severe Acute Respiratory Syndrome Coronavirus 2 (SARS-CoV-2) emerged in late 2019, swiftly sparking a widespread outbreak of Coronavirus Disease 2019 (COVID-19) [1]. The SARS-CoV-2 genome, approximately 30,000 nucleotides long, encodes nonstructural proteins through two large polyproteins, ORF1a and ORF1b, which assemble into the replication–transcription complex. The genome's final third codes for structural proteins: spike (S), envelope (E), membrane (M), and nucleocapsid (N) [2,3]. Reverse transcription

* Corresponding author. Institute of Preventive Medicine, National Defense Medical Center, Taipei, Taiwan.
E-mail address: tsghsun@gmail.com (J.-R. Sun).

https://doi.org/10.1016/j.heliyon.2025.e42503
Received 11 May 2024; Received in revised form 26 January 2025; Accepted 5 February 2025
Available online 6 February 2025

polymerase chain reaction (RT-PCR) is considered the gold standard for viral detection [4], using primers targeting ORF1ab, N, and E genes to assess pathogen detection reproducibility and sensitivity [5–7].

Upon host cell entry, SARS-CoV-2 begins a subgenome replication strategy, generating complementary negative-sense full-length RNA [8,9]. This process amplifies the plus-strand viral genomic RNA (gRNA) and transcribes a set of plus-strand subgenomic RNAs (sgRNA) with a common leader sequence fused to the gene sequences at the 5' end of the structural gene, which is essential for the viral replication lifecycle [8,10–12]. Since sgRNAs only form during active viral replication, their RT-PCR detection can reveal virus infectious particles.

Syrian golden hamsters and K18 promoter–driven human ACE2–expressing mice (K18-hACE2 mice) have been recognized as valuable rodent models for studying SARS-CoV-2 and assessing vaccine and therapeutic efficacies [13,14]. Studies have linked RT-PCR assays targeting both gRNAs and sgRNAs with viral culture outcomes in clinical specimens [6,9,11,14–16]. These studies suggest that PCR targeting gRNA may usually be insufficient, as gRNA remains detectable through RT-qPCR weeks after symptom onset in convalescent patients, even when viral cultures are negative. In contrast, sgRNAs offer more accurate markers of active viral replication. However, the effectiveness of these targets for measuring the viral load in rodents infected with SARS-CoV-2 is yet to be comparatively evaluated. Herein, we developed and evaluated novel RT-qPCR assays for quantifying gRNAs, sgRNAs, and rodent housekeeping genes to assess viral loads in infected rodents, offering a rapid alternative to traditional viral culture methods for future applications.

2. Materials and methods

2.1. Virus and cell culture

Experiments with live SARS-CoV-2 were conducted in a biosafety level 3 and animal biosafety level 3 laboratory at the Institute of Preventive Medicine (IPM), approved by the Taiwan Centers for Disease Control and Prevention. SARS-CoV-2 (human/TWN/CGMH-CGU-04/2020; GenBank number MT370517) was isolated in March 2020 from a COVID-19 patient in Wuhan, China [17]. It was cultured in Vero E6 cells (ATCC CRL-1586, Manassas, VA, USA) and stored at −80 °C in single-use aliquots.

2.2. RNA extraction and RT-qPCR assays

RT-qPCR targeted four SARS-CoV-2 regions: ORF1ab, N, E, and E-sgRNA, as illustrated in Fig. 1, with housekeeping genes *Gapdh* (for hamsters) and *Actb* (for mice) for normalization. The primers used in this study are listed in Table 1. Fragments were cloned into the pGEM-T Easy vector as the manufacturer's instructions (Promega, Madison, WI, USA), propagated in *Escherichia coli* DH10B, and stored at −80 °C. Plasmids were templates for further PCR amplification using T7 and SP6 primers. Amplified T7–SP6 PCR products were quantified using a NanoDrop spectrophotometer (Thermo Fisher Scientific) and verified with the Qubit dsDNA HS Assay Kit using Qubit 2.0 Fluorometer (Thermo Fisher Scientific, Waltham, MA, USA). The products were then serially diluted to create a standard curve. Total RNA was extracted from homogenized rodent specimens using TRIzol reagent (Thermo Fisher Scientific, Waltham, MA, USA), and cDNA was synthesized using the SuperScript IV first-strand synthesis system (Thermo Fisher Scientific, Waltham, MA, USA). The expression levels of the genes targeting ORF1ab, N, E, and E-sgRNA and the housekeeping genes were quantified using RT-qPCR assays on a LightCycler 480 II instrument (Roche Diagnostics GmbH, Mannheim, Germany). The RT-qPCR assays were conducted using the PowerTrack SYBR Green Master Mix, following the manufacturer's instructions. The thermal cycling conditions were as follows: initial pre-incubation at 50 °C for 2 min, followed by denaturation at 95 °C for 2 min; amplification over 45 cycles at 95 °C for 15 s, 56 °C for 15 s, and 60 °C for 40 s; melting curve analysis at 95 °C for 5 s and 65 °C for 1 min; and a final cooling step at 40 °C for 30 s. A standard curve for each target in the RT-qPCR assay was generated using a dilution series of 10^2–10^6 copies/reaction of the T7–SP6 PCR product. Viral load was quantified as viral RNA copies per 10^5 transcripts of hamster *Gapdh* or mouse *Actb*.

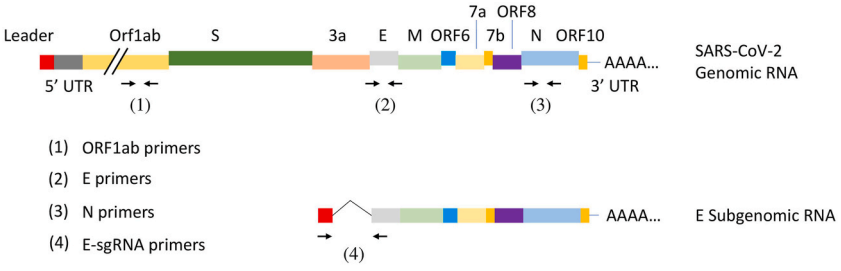

Fig. 1. Schematic representation of primer positions on the SARS-CoV-2 genome for RT-qPCR assays. The primer sets for the RT-qPCR assay for ORF1ab were designed on the primers for RT-qPCR assays for the E and N genes, which are designed to identify virion RNA, gRNA, and sgRNA. The E-sgRNA assay utilizes a forward primer specifically designed to target the leader sequence, thereby preventing the amplification of genomic RNA.

Table 1
Primers for RT-qPCR assays.

Target Region	Oligonucleotide	Sequencce (5′- 3′)	Reference
pGEM T plasmid	T7_promoter-F	TAATACGACTCACTATAGGG	
	SP6_promoter-R	ATTTAGGTGACACTATAGAA	
ORF1ab	SARSCoV2_ORF1ab-F	CCCTGTGGGTTTTACACTTAA	(5)
	SARSCoV2_ORF1ab-R	ACGATTGTGCATCAGCTGA	
Nucleocapsid (N)	SARSCoV2_N-F	GCCTCTTCTCGTTCCTCATCAC	(7)
	SARSCoV2_N-R	AGCAGCATCACCGCCATTG	
Envelope (E)	E_Sarbeco_F	ACAGGTACGTTAATAGTTAATAGCGT	(6)
	E_Sarbeco_R	ATATTGCAGCAGTACGCACACA	
Subgenomic Envelope (E)	sgLeadSARSCoV2-F	CGATCTCTTGTAGATCTGTTCTC	(6)
	E_Sarbeco_R	ATATTGCAGCAGTACGCACACA	
Gapdh (hamster)	Hamster_G3pdhQPCR_F	GACATCAAGAAGGTGGTGAAGC	(20)
	Hamster_G3pdhQPCR_R	CATCAAAGGTGGAAGAGTGGGA	
Actb (Mouse)	Mouse_β_Actin_F	GGCTGTATTCCCCTCCATCG	(21)
	Mouse_β_Actin_R	CCAGTTGGTAACAATGCCATGT	

2.3. Reproducibility and limit of detection of RT-qPCR assays

Ten-fold serial dilutions of the reference standard ranging from 10^6 to 10^2 copies/μL were performed in triplicate to determine intra- and inter-assay reproducibility. The intra-assay reproducibility was evaluated by analyzing triplicate samples within the same run, while the inter-assay reproducibility was tested across 3 separate days within a week. The variability in Ct values was assessed to determine consistency. A coefficient of variation <5 % indicates high reproducibility [18]. Ten-fold serial dilutions of the reference standard, ranging from 10^6 to 1 copies/μL, were employed in the real-time PCR assay in ten replications to confirm its analytical sensitivity [19].

2.4. Viral load detection in rodent lung tissues

The protocol was approved by the Institutional Animal Care and Use Committee of the IPM. Residual lung tissues from 42 Syrian hamsters and 60 K18-hACE2 mice infected with SARS-CoV-2 were obtained from the core facility platform for emerging infectious disease research at the National Core Facility for Biopharmaceuticals to evaluate the efficacy of our RT-qPCR assays in determining the viral load. All samples were obtained from animals used in SARS-CoV-2 challenge experiments, including four mock-infected controls. Residual lung tissues were collected and stored at 4 °C for processing procedures within 4–10 h. These tissues were placed into screw-

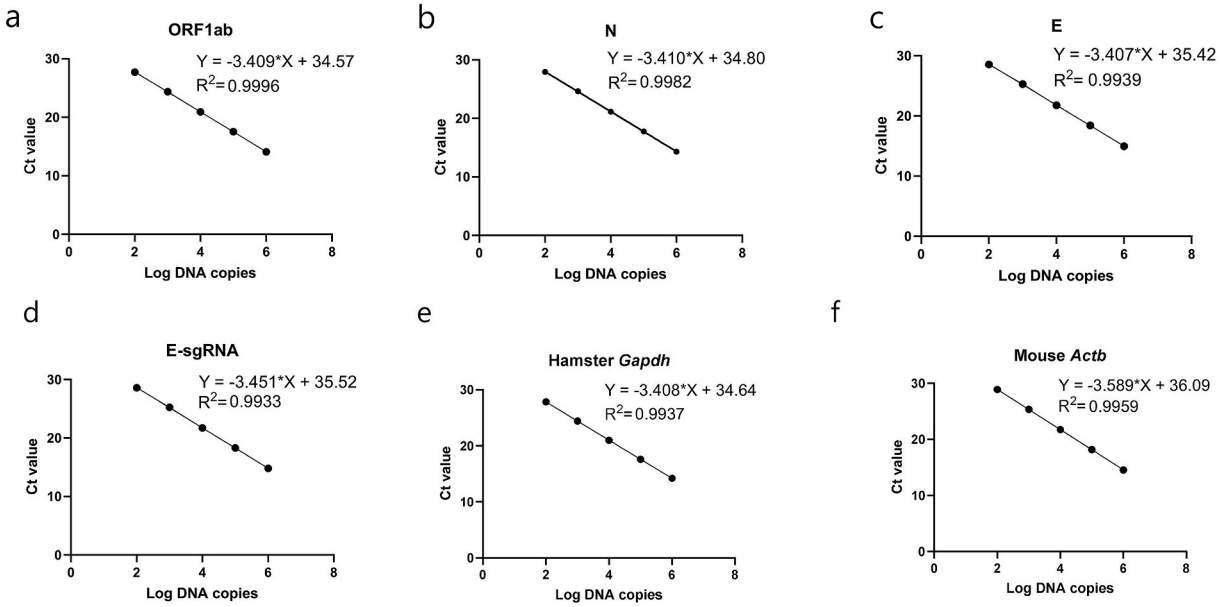

Fig. 2. Efficiency and linearity of RT-PCR assays for SARS-CoV-2 and rodent housekeeping genes using T7–SP6 PCR products. (a) ORF1ab, (b) N, (c) E, (d) E-sgRNA, (e) Hamster *Gapdh*, and (f) Mice *Actb*. The plots show the mean cycle threshold (Ct value) values in relation to logarithmic DNA copy numbers (Log DNA copies), complemented by the associated correlation coefficients and regression equations, showcasing the assay's analytical precision.

capped tubes with silica beads and Dulbecco's Modified Eagle Medium (DMEM) (Thermo Fisher Scientific, Waltham, MA, USA) and then homogenized using a Bertin Instruments tissue homogenizer (France). Homogenates underwent viral culture and RNA extraction, with cell exposure to serial dilutions in DMEM. Vero E6 cells (4×10^5/well) were seeded in 12-well culture plates. The cells were subsequently exposed to serial dilutions of the specimens and incubated in DMEM supplemented with 0.3 % agarose (Invitrogen, Waltham, MA, USA) at 37 °C in a 5 % CO_2 atmosphere. Daily observation of the cytopathic effects continued until the manifestation of individual plaques. After a 3-day incubation, the cells were fixed with a 4 % paraformaldehyde solution (v/v) for 1 h at room temperature. Staining was then performed using a 0.5 % crystal violet solution (w/v) for 30 min.

2.5. Statistical analyses

Statistical analyses were performed using the SPSS version 27 software package (SPSS Inc., IBM Company, Chicago, IL, USA). The diagnostic performance regarding sensitivity, specificity, positive predictive values (PPV), and negative predictive values (NPV) of our RT-qPCR assays was determined through comparison, with viral culture as the gold standard. Sensitivity is defined as the proportion of true positive results and is calculated by dividing the number of samples positive using RT-qPCR and viral culture by the total number of viral culture-positive samples. Specificity is defined as the proportion of true negative results, and it is calculated by dividing the number of samples negative using RT-qPCR and viral culture by the total number of viral culture-negative samples. The correlation between the RT-qPCR assay outcomes and viral culture results was analyzed using Pearson's correlation coefficients to detect monotonic relationships. Regression lines and violin plot were plotted using GraphPad Prism version 9 (GraphPad Software, San Diego, CA, USA) to visualize the data.

3. Results

3.1. Precision of RT-qPCR assays

The amplification efficiencies for the ORF1ab, N, E, E-sgRNA, Hamster *Gapdh*, and Mice *Actb* genes were 96 %, 96 %, 97 %, 95 %,

Table 2
Intra- and inter-assay reproducibility of the RT-qPCR assays.

Reference standard		intra-assay				inter-assay			
	(copies/μL)	Ct (mean ± SD)			CV%	Ct (mean ± SD)			CV%
ORF1ab	10^6	14.14	±	0.00	0.03 %	13.97	±	0.15	1.06 %
	10^5	17.54	±	0.00	0.03 %	17.41	±	0.19	1.08 %
	10^4	20.92	±	0.03	0.14 %	20.84	±	0.16	0.76 %
	10^3	24.46	±	0.02	0.08 %	24.39	±	0.14	0.57 %
	10^2	27.85	±	0.06	0.21 %	27.62	±	0.03	0.11 %
N	10^6	14.92	±	0.04	0.25 %	14.83	±	0.23	1.54 %
	10^5	18.98	±	0.03	0.15 %	18.30	±	0.30	1.66 %
	10^4	22.67	±	0.03	0.12 %	21.74	±	0.29	1.33 %
	10^3	25.75	±	0.05	0.19 %	25.19	±	0.28	1.12 %
	10^2	29.31	±	0.21	0.70 %	28.64	±	0.38	1.31 %
E	10^6	15.19	±	0.01	0.08 %	15.33	±	0.17	1.12 %
	10^5	18.67	±	0.00	0.00 %	18.78	±	0.13	0.67 %
	10^4	22.08	±	0.01	0.04 %	22.18	±	0.19	0.87 %
	10^3	25.57	±	0.05	0.19 %	25.67	±	0.13	0.50 %
	10^2	29.18	±	0.29	1.00 %	29.29	±	0.29	0.98 %
E-sgRNA	10^6	15.08	±	0.01	0.05 %	15.20	±	0.07	0.44 %
	10^5	18.63	±	0.01	0.04 %	18.65	±	0.12	0.67 %
	10^4	22.04	±	0.02	0.11 %	22.13	±	0.13	0.58 %
	10^3	25.60	±	0.02	0.10 %	25.60	±	0.08	0.30 %
	10^2	28.87	±	0.25	0.86 %	29.14	±	0.29	0.98 %
Hamster *Gapdh*	10^6	14.28	±	0.02	0.13 %	14.67	±	0.22	1.52 %
	10^5	17.70	±	0.06	0.32 %	17.99	±	0.23	1.30 %
	10^4	21.06	±	0.08	0.37 %	21.43	±	0.28	1.30 %
	10^3	24.55	±	0.03	0.12 %	24.86	±	0.24	0.96 %
	10^2	27.97	±	0.15	0.53 %	28.42	±	0.31	1.08 %
Mouse*Actb*	10^6	13.97	±	0.11	0.82 %	13.36	±	0.17	1.30 %
	10^5	17.76	±	0.12	0.69 %	16.97	±	0.14	0.82 %
	10^4	21.57	±	0.13	0.63 %	20.74	±	0.15	0.72 %
	10^3	25.18	±	0.18	0.72 %	24.57	±	0.39	1.60 %
	10^2	28.88	±	0.23	0.79 %	28.25	±	0.42	1.49 %

97 %, and 90 %, respectively (Fig. 2). The linear correlation (R^2) between cycle threshold (Ct) values and the logarithm of copy numbers for these genes ranged from 0.9933 to 0.9996. Intra-assay precision for Ct values demonstrated low variation: ORF1ab (0.03%–0.21 %), N (0.12%–0.7 %), E (0.08%–1%), E-sgRNA (0.05%–0.86 %), Hamster *Gapdh* (0.12%–0.53 %), and Mice *Actb* (0.63%–0.82 %). Inter-assay precision also exhibited minimal variation: ORF1ab (0.57%–1.08 %), N (1.12%–1.66 %), E (0.5%–1.12 %), E-sgRNA (0.3%–0.98 %), Hamster *Gapdh* (0.96%–1.52 %), and Mouse *Actb* genes (0.72%–1.6 %) (Table 2). The analytical sensitivity of the RT-qPCR assay was evaluated by determining the limit of detection (LOD) for each gene target. Across 10 runs, the assays revealed a mean LOD of 1–10 copies per microliter (Table 3).

3.2. Performance evaluation of rodent lung tissues

Viral culture outcomes from SARS-CoV-2-infected rodent lung homogenates identified 39 positive and three negative cases in hamster samples and 37 positive and 23 negative cases in mouse samples. The median viral loads were 6.1×10^5 pfu/mL in hamster samples (range: 3.5×10^2 to 2.7×10^7 pfu/mL) and 6.8×10^3 pfu/mL in K18-hACE2 mice samples (range: 40–2.4×10^6 pfu/mL). These results served as benchmarks for assessing RT-qPCR diagnostic efficacy (Tables 4 and 5). In hamsters, the qRT-PCR assays demonstrated sensitivities of 1.0 for ORF1ab, N, and E genes, and 0.97 for E-sgRNA, with specificities of 1.0 for ORF1ab, N, and E-sgRNA, but 0.67 for E. In K18-hACE2 mice, sensitivities were 1.0 for ORF1ab, N, and E, but 0.92 for E-sgRNA, while specificities were 0.39 for ORF1ab, 0.61 for N, 0.61 for E, and 0.96 for E-sgRNA.

3.3. Viral load detection performance of RT-qPCR assays

To further evaluate the effectiveness of viral load detection using RT-qPCR assays, the copy numbers quantified using the four RT-qPCR assays (ORF1ab, N, E, E-sgRNA) were normalized against cellular transcripts, and the results were compared to plaque-forming units from viral cultures (Fig. 3). Viral copies per cellular transcript correlated significantly with culture results, showing R^2 values between 0.809 and 0.864 (Fig. 3). To quantify the RT-qPCR assay targets within the samples, we analyzed RT-qPCR positive specimens from both mice and hamsters for copies of ORF1ab, N, and E-sgRNA, using the E gene as a reference for comparison. The relative quantification ratio median for ORF1ab, N, and E-sgRNA were 0.25, 1.0, and 0.12, respectively, normalized against E as the baseline (Fig. 4). The analysis indicated a strong correlation between the RT-qPCR detection of the ORF1ab, N, E, and E-sgRNA genes and viral culture results, with Pearson's correlation coefficients ranging from 0.90 to 0.93 (Table 6). Notably, the E-sgRNA RT-qPCR assay exhibited the strongest correlation with the viral load among all evaluated targets.

4. Discussion

The accurate quantification of virus levels is essential for SARS-CoV-2 vaccine and therapeutic studies in animal models. While plaque assays and TCID50 are standard methods, they are labor-intensive and require BSL-3 laboratories. Quantitative PCR assays, which are used to detect viral RNA, offer a more efficient alternative for measuring viral loads. In this study, we developed and validated RT-qPCR assays targeting gRNA, sgRNAs, and rodent housekeeping genes suitable for detecting and quantifying SARS-CoV-2 in rodent lungs. The six primer pairs used for virus detection and cellular housekeeping gene quantification have been widely employed in earlier studies targeting these markers, proving their efficacy in SARS-CoV-2 detection in human and primate samples as well as in cellular infection assays [5–7,20,21]. We demonstrated that all RT-qPCR assays were capable of detecting as few as 10 copies/μL of the DNA fragment carrying the target sequence in our study, with a consistent linear detection range spanning 10^2 to 10^6 orders of magnitude ($R^2 > 0.99$ for all).

Quantifying the SARS-CoV-2 viral load is crucial for identifying severe infections, monitoring disease progression, and evaluating treatment efficacy [22,23]. Although viral culture is the standard, it is laborious and slow. The Ct value, determined using RT-qPCR assays, serves as an efficient alternative to viral load assessment [24,25]. However, the accuracy of the Ct values may be compromised by batch conditions and enzyme activity. An interlaboratory survey involving 800 laboratories noted a median Ct value of 14 cycles with variations up to three cycles on the same analytical platform [23]. We used serial dilutions of T7–SP6 PCR products to generate a standard curve, enabling precise quantification with minimal inter- and intra-run variations. While *in vitro*-transcribed RNA templates

Table 3
Limit of detection of RT-qPCR in each gene target. The results are presented as the number of positive detections out of 10 trials at each concentration level.

	Positive/tested (%)					
Standard sample (copies/μl)	Orf1ab	N	E	E-sgRNA	Hamster *Gapdh*	Mouse *Actb*
10^6	10/10	10/10	10/10	10/10	10/10	10/10
10^5	10/10	10/10	10/10	10/10	10/10	10/10
10^4	10/10	10/10	10/10	10/10	10/10	10/10
10^3	10/10	10/10	10/10	10/10	10/10	10/10
10^2	10/10	10/10	10/10	10/10	10/10	10/10
10	10/10	10/10	10/10	10/10	10/10	10/10
1	9/10	6/10	6/10	5/10	8/10	9/10

Table 4
The diagnostic performance of RT-qPCR assays in hamster lung tissue.

RT-qPCR assay		Viral culture		Sensitivity (%) (95%CI[a])	Specificity (%) (95%CI)	PPV[b] (%) (95%CI)	NPV[c] (%) (95%CI)
		Positive	Negative				
ORF1ab	Positive	39	0	1.0 (0.95–1.0)	1.0 (0.37–1.0)	1.0 (0.95–1.0)	1.0 (0.37–1.0)
	Negative	0	3				
N	Positive	39	0	1.0 (0.95–1.0)	1.0 (0.37–1.0)	1.0 (0.95–1.0)	1.0 (0.37–1.0)
	Negative	0	3				
E	Positive	39	1	1.0 (0.96–1.0)	0.67 (0.66–1.0)	0.98 (0.94–0.98)	1.00 (0.22–1.0)
	Negative	0	2				
E-sgRNA	Positive	38	0	0.97 (0.92–0.97)	1.00 (0.35–1.0)	1.00 (0.95–1.0)	0.75 (0.26–0.75)
	Negative	1	3				

[a] CI, confidence interval.
[b] PPV, positive predictive value.
[c] NPV, negative predictive value.

Table 5
The diagnostic performance of RT-qPCR assays in K18-hACE2 mice lung tissue.

RT-qPCR assay		Viral culture		Sensitivity (%) (95%CI)	Specificity (%) (95%CI)	PPV (%) (95%CI)	NPV (%) (95%CI)
		Positive	Negative				
ORF1ab	Positive	37	14	1.0 (0.92–1.0)	0.39 (0.26–0.39)	0.73 (0.67–0.73)	1.0 (0.66–1.0)
	Negative	0	9				
N	Positive	37	9	1.0 (0.92–1.0)	0.61 (0.47–0.61)	0.84 (0.73–0.8)	1.0 (0.77–1.0)
	Negative	0	14				
E	Positive	37	9	1.0 (0.92–1.0)	0.61 (0.47–0.61)	0.84 (0.73–0.8)	1.0 (0.77–1.0)
	Negative	0	14				
E-sgRNA	Positive	34	1	0.92 (0.92–1.0)	0.96 (0.83–0.96)	0.97 (0.90–0.97)	0.88 (0.87–1.0)
	Negative	3	22				

used for standard curves offer high sensitivity and specificity, their fragility complicates preservation [25]. The T7–SP6 PCR product, which is DNA, is more stable than *in vitro*-transcribed RNA and can be preserved for at least 6 months in a refrigerator. Consequently, we recommend the use of DNA templates as a basis for standard curves in RT-qPCR quantification experiments, particularly in the absence of internationally recognized quantitative standards.

Various forms of viral RNA are detectable in lung homogenates infected with SARS-CoV-2, including virion-encapsulated genomic RNA (virion RNA), positive- and negative-sense genomic RNA (gRNA), and subgenomic RNA (sgRNA) [13,26,27]. Virion RNA/gRNA is approximately tenfold more abundant than sgRNA, and the ratio of positive-sense to negative-sense gRNA exceeds 150-fold [26]. In our study, the copy number of ORF1ab was about one-quarter that of the E gene, while E-sgRNA constituted only 10 %. The N gene copy number was comparable to that of the E gene (Fig. 4). The underlying causes of these ratios merit additional investigation. The specificity for detecting gRNA targets, such as ORF1ab, N, and E genes, in K18-hACE2 mice was lower than that in hamsters, possibly owing to a higher number of viral culture-negative samples that tested positive for these genes using RT-qPCR (Tables 4 and 5). In contrast, RT-qPCR results for sgRNA detection were consistently accurate in hamsters and K18-hACE2 mice. The residual samples used for validating RT-qPCR assay performance exhibited varying sacrifice time points post-infection, attributed to differences in study design and sample sources. Nevertheless, these findings suggest that the observed discrepancy may result from residual viral RNA in K18-hACE2 lung tissue rather than active viral replication.

Combining these assays enhances sensitivity and aids in studying viral pathogenesis and disease severity in infected organs. Multiple clinical studies link sgRNA levels with successful viral culture in cell cultures, suggesting that sgRNA is a marker of active viral replication [6,9,28,29]. However, this finding is not universally supported, with some studies indicating that sgRNA does not reliably indicate active replication [14,30,31]. In clinical specimens, the limited cellular material in the sputum or nasopharyngeal swabs may result in a low abundance of sgRNAs. Additionally, the presence of inhibitors can compromise the accuracy of sgRNA detection [14, 32]. To date, the only animal study involving rhesus macaques infected with SARS-CoV-2 has compared the detection efficiencies of sgRNA and gRNA. This demonstrated that sgRNA levels decline before gRNA levels do, allowing for a more timely and precise measurement of the effectiveness of antibody treatment [6]. Our research marks the first comparison of the quantitative accuracy of gRNA target (E) and sgRNA target (Sub-E) assays in a rodent model infected with SARS-CoV-2. Although all four RT-qPCR assays demonstrated high sensitivity, our findings suggest that sgRNA measurement may offer a more precise indicator of viral replication in rodent models.

To quantify the RT-qPCR analysis of rodent lung samples, instead of directly calculating Ct values, we estimated the viral copies using the housekeeping gene normalization method to minimize errors. Normalization based on lung tissue weight for viral load per gram (g) can lead to significant inaccuracies because of the small size of lung sections [32]. Therefore, we used the same volume of cDNA for the simultaneous viral and housekeeping gene assays (*Gapdh* for hamsters and *Actb* for mice), thereby achieving accurate copy numbers. Finally, normalization of viral copies against 10^5 cellular transcripts was performed to represent the viral load in the

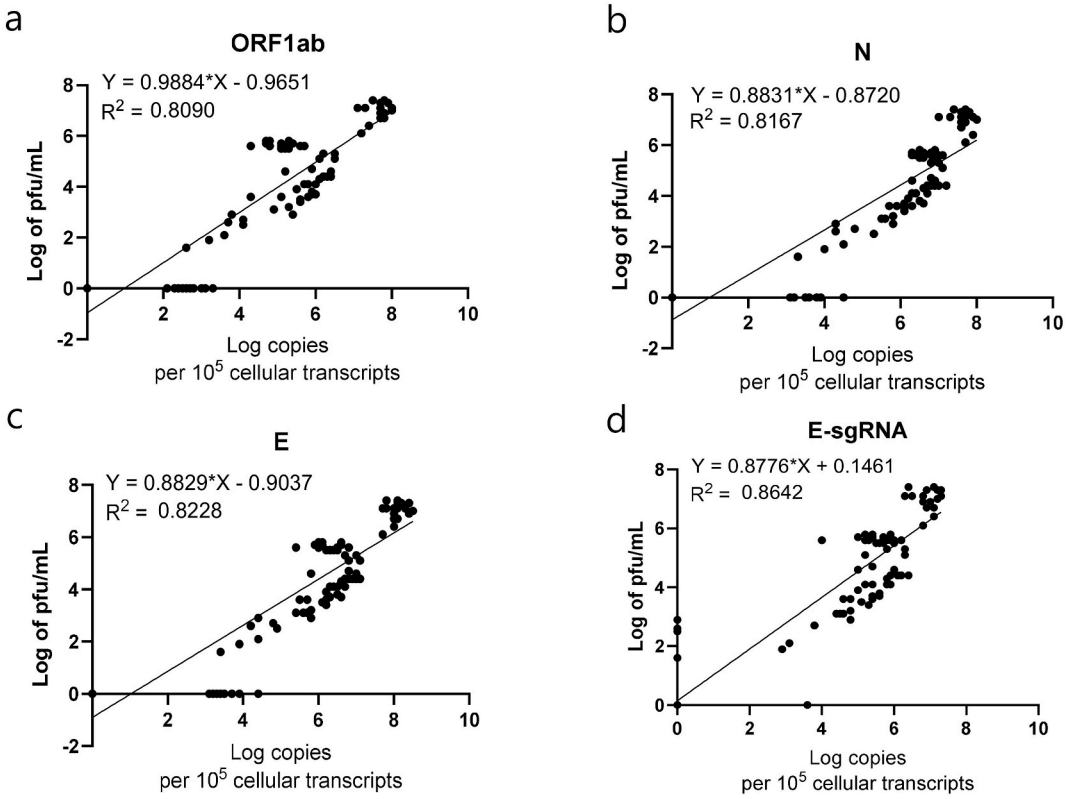

Fig. 3. Linear regression Analysis of RT-qPCR assays and viral loads detected by viral culture. (a) ORF1ab, (b)N, (c) E, and (d) Esg-RNA. The graph illustrates the logarithm of pfu/mL values corresponding to normalized copy numbers, along with the respective correlation coefficients and regression equations.

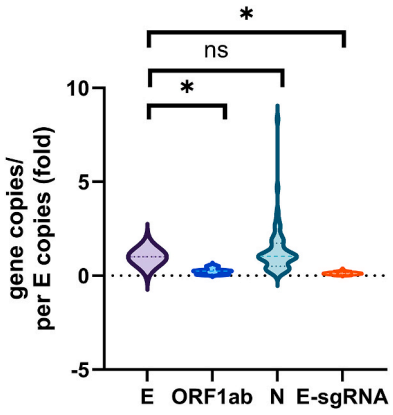

Fig. 4. Quantification of viral copy numbers relative to the E gene. The RT-qPCR positive samples from both mice and hamsters were analyzed for copies of ORF1ab, N, and E-sgRNA, with comparisons made to E. Statistical analysis was performed using the Kruskal-Wallis test. The asterisk indicates a p-value <0.001.

lung tissue, as previously described [33]. In this study, we observed that the four RT-qPCR assay sets exhibited a high correlation between gRNA and sgRNA, which is consistent with the findings of previous studies [28,34,35]. Among the four RT-qPCR assay sets, E-sgRNA showed the strongest correlation with viral infectivity. We suggest that E-sgRNA offers a more precise depiction of actively replicating viruses in viral culture.

In conclusion, four RT-qPCR assays that enable sensitive detection of SARS-CoV-2 were developed and validated in this study. The construction of quantitative curves demonstrated that these PCR assays were capable of effectively detecting low viral loads. These RT-qPCR assays utilize housekeeping gene normalization, offering a viable alternative to viral culture for quantifying viral release from

Table 6
Correlation of Viral culture and RT-qPCR assays.

Target	Pearson's correlation coefficient (p-value)				
	Viral culture	ORF1ab	N	E	E-sgRNA
Viral culture	1				
ORF1ab	0.90 (<0.001)	1			
N	0.90 (<0.001)	0.95 (<0.001)	1		
E	0.91 (<0.001)	0.95 (<0.001)	0.97 (<0.001)	1	
E-sgRNA	0.93 (<0.001)	0.92 (<0.001)	0.92 (<0.001)	0.92 (<0.001)	1

homogenized tissues in rodent models. While the assay targeting gRNA detected higher copy numbers, our results showed that assays targeting E-sgRNA correlated better with the culture results compared with the other targets. Thus, sgRNAs may serve as accurate indicators of active viral replication in rodent models.

CRediT authorship contribution statement

Yun-Hsiang Cheng: Writing – original draft, Project administration, Methodology, Funding acquisition, Formal analysis. **Cheng-Hsiu Chen:** Visualization, Validation, Methodology. **Ping-Cheng Liu:** Resources, Methodology, Formal analysis. **Wen-Ting Chen:** Visualization, Validation. **Chi-Ju Hsu:** Visualization, Validation, Software, Methodology. **Cheng-Cheung Chen:** Resources, Funding acquisition. **Jun-Ren Sun:** Writing – review & editing, Writing – original draft, Validation, Supervision, Resources, Methodology, Funding acquisition, Formal analysis, Conceptualization.

Data availability statement

All data included in the article. The essential materials supporting this article will be shared on reasonable request to the corresponding author.

Funding

This work was supported by grants from the Ministry of National Defense, R.O.C. (MND-MAB-D-113172, MND-MAB-C04-112016, MND-MAB-D-111104, MND-MAB-110-065, MND-MAB-D-114183, and MND-MAB-D-114185) and the National Science and Technology Council in Taiwan (NSTC 111-2320-B-016-014, NSTC 111-2321-B-016-002, NSTC 111-2740-B-016 -001, NSTC 112-2320-B-016-007, NSTC 112-2321-B-016 -002, NSTC 112-2740-B-016 -001,NSTC 113-2740-B-016 -001, and NSTC 113-2321-B-016-002).

Declaration of competing interest

The authors declare that they have no known competing financial interests or personal relationships that could have appeared to influence the work reported in this paper.

Acknowledgements

The animal study protocol was approved by the Institutional Animal Care and Use Committee of IPM. IACUC number: AN-110-13. We thank the technical services provided by the "Core facility platform for emerging infectious disease research of the National Core Facility for Biopharmaceuticals, National Science and Technology Council, Taiwan". We also thank National Laboratory Animal Center (NLAC), NARLabs, Taiwan, for technical support in pathological service.

References

[1] N. Zhu, D. Zhang, W. Wang, X. Li, B. Yang, J. Song, X. Zhao, B. Huang, W. Shi, R. Lu, P. Niu, F. Zhan, X. Ma, D. Wang, W. Xu, G. Wu, G.F. Gao, W. Tan, A novel coronavirus from patients with pneumonia in China, 2019, N. Engl. J. Med. 382 (2020) 727–733.
[2] F. Wu, S. Zhao, B. Yu, Y.M. Chen, W. Wang, Z.G. Song, Y. Hu, Z.W. Tao, J.H. Tian, Y.Y. Pei, M.L. Yuan, Y.L. Zhang, F.H. Dai, Y. Liu, Q.M. Wang, J.J. Zheng, L. Xu, E.C. Holmes, Y.Z. Zhang, A new coronavirus associated with human respiratory disease in China, Nature 579 (2020) 265–269.
[3] R. Yadav, J.K. Chaudhary, N. Jain, P.K. Chaudhary, S. Khanra, P. Dhamija, A. Sharma, A. Kumar, S. Handu, Role of structural and non-structural proteins and therapeutic targets of SARS-CoV-2 for COVID-19, Cells 10 (2021) 821.
[4] H. Tombuloglu, H. Sabit, H. Al-Khallaf, J.H. Kabanja, M. Alsaeed, N. Al-Saleh, E. Al-Suhaimi, Multiplex real-time RT-PCR method for the diagnosis of SARS-CoV-2 by targeting viral N, RdRP and human RP genes, Sci. Rep. 12 (2022) 2853.
[5] Y. Xu, X. Li, B. Zhu, H. Liang, C. Fang, Y. Gong, Q. Guo, X. Sun, D. Zhao, J. Shen, H. Zhang, H. Liu, H. Xia, J. Tang, K. Zhang, S. Gong, Characteristics of pediatric SARS-CoV-2 infection and potential evidence for persistent fecal viral shedding, Nat. Med. 26 (2020) 502–505.
[6] G. Dagotto, N.B. Mercado, D.R. Martinez, Y.J. Hou, J.P. Nkolola, R.H. Carnahan, J.E. Crowe Jr., R.S. Baric, D.H. Barouch, Comparison of subgenomic and total RNA in SARS-CoV-2 challenged rhesus macaques, J. Virol. 95 (2021) e02370.
[7] M. Cortese, J.Y. Lee, B. Cerikan, C.J. Neufeldt, V.M.J. Oorschot, S. Köhrer, J. Hennies, N.L. Schieber, P. Ronchi, G. Mizzon, I. Romero-Brey, R. Santarella-Mellwig, M. Schorb, M. Boermel, K. Mocaer, M.S. Beckwith, R.M. Templin, V. Gross, C. Pape, C. Tischer, J. Frankish, N.K. Horvat, V. Laketa, M. Stanifer, S. Boulant, A. Ruggieri, L. Chatel-Chaix, Y. Schwab, R. Bartenschlager, Integrative imaging reveals SARS-CoV-2-induced reshaping of subcellular morphologies, Cell Host Microbe 28 (2020) 853–866.e5.

[8] D. Kim, J.Y. Lee, J.S. Yang, J.W. Kim, V.N. Kim, H. Chang, The architecture of SARS-CoV-2 transcriptome, Cell 181 (2020) 914–921.e10.
[9] Z. Chen, R.W.Y. Ng, G. Lui, L. Ling, C. Chow, A.C.M. Yeung, S.S. Boon, M.H. Wang, K.C.C. Chan, R.W.Y. Chan, D.S.C. Hui, P.K.S. Chan, Profiling of SARS-CoV-2 subgenomic RNAs in clinical specimens, Microbiol. Spectr. 10 (2022) e0018222.
[10] Y. Zhang, X. Zhang, H. Zheng, L. Liu, Subgenomic RNAs and their encoded proteins contribute to the rapid duplication of SARS-CoV-2 and COVID-19 progression, Biomolecules 12 (2022) 1680.
[11] F. Roesmann, I. Jakobsche, C. Pallas, A. Wilhelm, J. Raffel, N. Kohmer, T. Toptan, A. Berger, U. Goetsch, S. Ciesek, M. Widera, Comparison of the Ct-values for genomic and subgenomic SARS-CoV-2 RNA reveals limited predictive value for the presence of replication competent virus, J. Clin. Virol. 165 (2023) 105499.
[12] I. Sola, F. Almazán, S. Zúñiga, L. Enjuanes, Continuous and discontinuous RNA synthesis in coronaviruses, Annu Rev Virol 2 (2015) 265–288.
[13] H. Jeong, Y. Woo Lee, I.H. Park, H. Noh, S.H. Kim, J. Kim, D. Jeon, H.J. Jang, J. Oh, D. On, C. Uhm, K. Cho, H. Oh, S. Yoon, J.S. Seo, J.J. Kim, S.H. Seok, Y.J. Lee, S.M. Hong, S.H. An, S. Yeon Kim, Y.B. Kim, J.Y. Hwang, H.J. Lee, H.B. Kim, D.G. Jeong, D. Song, M. Song, M.S. Park, K.S. Choi, J.W. Park, J.Y. Seo, J.W. Yun, J. S. Shin, H.Y. Lee, K.T. Nam, J.K. Seong, Comparison of the pathogenesis of SARS-CoV-2 infection in K18-hACE2 mouse and Syrian golden hamster models, Dis Model Mech 15 (2022).
[14] S. Alexandersen, A. Chamings, T.R. Bhatta, SARS-CoV-2 genomic and subgenomic RNAs in diagnostic samples are not an indicator of active replication, Nat. Commun. 11 (2020) 6059.
[15] R. Wölfel, V.M. Corman, W. Guggemos, M. Seilmaier, S. Zange, M.A. Müller, D. Niemeyer, T.C. Jones, P. Vollmar, C. Rothe, M. Hoelscher, T. Bleicker, S. Brünink, J. Schneider, R. Ehmann, K. Zwirglmaier, C. Drosten, C. Wendtner, Virological assessment of hospitalized patients with COVID-2019, Nature 581 (2020) 465–469.
[16] Scola B. La, M. Le Bideau, J. Andreani, V.T. Hoang, C. Grimaldier, P. Colson, P. Gautret, D. Raoult, Viral RNA load as determined by cell culture as a management tool for discharge of SARS-CoV-2 patients from infectious disease wards, Eur. J. Clin. Microbiol. Infect. Dis. 39 (2020) 1059–1061.
[17] J.T. Wang, Y.Y. Lin, S.Y. Chang, S.H. Yeh, B.H. Hu, P.J. Chen, S.C. Chang, The role of phylogenetic analysis in clarifying the infection source of a COVID-19 patient, J. Infect. 81 (2020) 147–178.
[18] T-b Yang, J. Liu, J. Chen, Compared with conventional PCR assay, qPCR assay greatly improves the detection efficiency of predation, Ecol. Evol. 10 (2020) 7713–7722.
[19] Q. Zhang, R. Hu, Z. Gu, A real-time PCR assay for detection of emerging infectious *Elizabethkingia miricola*, Mol. Cell. Probes 52 (2020) 101571.
[20] C.-J. Hsu, W.-C. Lin, Y.-C. Chou, C.-M. Yang, H.-L. Wu, Y.-H. Cheng, P.-C. Liu, J.-Y. Chang, H.-Y. Chen, J.-R. Sun, P. Pelka, Dynamic changes of the blood chemistry in Syrian hamsters post-acute COVID-19, Microbiol. Spectr. 10 (2022) e02362, 21.
[21] S. Omori, T.-W. Wang, Y. Johmura, T. Kanai, Y. Nakano, T. Kido, E.A. Susaki, T. Nakajima, S. Shichino, S. Ueha, M. Ozawa, K. Yokote, S. Kumamoto, A. Nishiyama, T. Sakamoto, K. Yamaguchi, S. Hatakeyama, E. Shimizu, K. Katayama, Y. Yamada, S. Yamazaki, K. Iwasaki, C. Miyoshi, H. Funato, M. Yanagisawa, H. Ueno, S. Imoto, Y. Furukawa, N. Yoshida, K. Matsushima, H.R. Ueda, A. Miyajima, M. Nakanishi, Generation of a p16 reporter mouse and its use to characterize and target p16high cells in vivo, Cell Metab. 32 (2020) 814–828.e6.
[22] M.J. Lee, Quantifying SARS-CoV-2 viral load: current status and future prospects, Expert Rev. Mol. Diagn 21 (2021) 1017–1023.
[23] D. Rhoads, D.R. Peaper, R.C. She, F.S. Nolte, C.M. Wojewoda, N.W. Anderson, B.S. Pritt, College of American pathologists (CAP) microbiology committee perspective: caution must Be used in interpreting the cycle threshold (Ct) value, Clin. Infect. Dis. 72 (2021) e685–e686.
[24] R. de Kock, M. Baselmans, V. Scharnhorst, B. Deiman, Sensitive detection and quantification of SARS-CoV-2 by multiplex droplet digital RT-PCR, Eur. J. Clin. Microbiol. Infect. Dis. 40 (2021) 807–813.
[25] J. Bland, A. Kavanaugh, L.K. Hong, S.S. Kadkol, Development and validation of viral load assays to quantitate SARS-CoV-2, J Virol Methods 291 (2021) 114100.
[26] D. Kim, J.Y. Lee, J.S. Yang, J.W. Kim, V.N. Kim, H. Chang, The architecture of SARS-CoV-2 transcriptome, Cell 181 (2020) 914–921, e10.
[27] X. Ge, H. Zhou, F. Shen, G. Yang, Y. Zhang, X. Zhang, H. Li, SARS-CoV-2 subgenomic RNA: formation process and rapid molecular diagnostic methods, Clin. Chem. Lab. Med. (2023), https://doi.org/10.1515/cclm-2023-0846.
[28] R. Perera, E. Tso, O.T.Y. Tsang, D.N.C. Tsang, K. Fung, Y.W.Y. Leung, A.W.H. Chin, D.K.W. Chu, S.M.S. Cheng, L.L.M. Poon, V.W.M. Chuang, M. Peiris, SARS-CoV-2 virus culture and subgenomic RNA for respiratory specimens from patients with mild coronavirus disease, Emerg. Infect. Dis. 26 (2020) 2701–2704.
[29] M. Santos Bravo, C. Berengua, P. Marin, M. Esteban, C. Rodriguez, M. Del Cuerpo, E. Miro, G. Cuesta, M. Mosquera, S. Sanchez-Palomino, J. Vila, N. Rabella, M. A. Marcos, Viral culture confirmed SARS-CoV-2 subgenomic RNA value as a good surrogate marker of infectivity, J. Clin. Microbiol. 60 (2022) e0160921.
[30] R. Verma, E. Kim, G.J. Martinez-Colon, P. Jagannathan, A. Rustagi, J. Parsonnet, H. Bonilla, C. Khosla, M. Holubar, A. Subramanian, U. Singh, Y. Maldonado, C. A. Blish, J.R. Andrews, SARS-CoV-2 subgenomic RNA kinetics in longitudinal clinical samples, Open Forum Infect. Dis. 8 (2021) ofab310.
[31] D.E. Dimcheff, A.L. Valesano, K.E. Rumfelt, W.J. Fitzsimmons, C. Blair, C. Mirabelli, J.G. Petrie, E.T. Martin, C. Bhambhani, M. Tewari, Severe acute respiratory syndrome coronavirus 2 total and subgenomic RNA viral load in hospitalized patients, J. Infect. Dis. 224 (2021) 1287–1293.
[32] K.A. Ryan, K.R. Bewley, S.A. Fotheringham, G.S. Slack, P. Brown, Y. Hall, N.I. Wand, A.C. Marriott, B.E. Cavell, J.A. Tree, L. Allen, M.J. Aram, T.J. Bean, E. Brunt, K.R. Buttigieg, D.P. Carter, R. Cobb, N.S. Coombes, S.J. Findlay-Wilson, K.J. Godwin, K.E. Gooch, J. Gouriet, R. Halkerston, D.J. Harris, T.H. Hender, H. E. Humphries, L. Hunter, C.M.K. Ho, C.L. Kennard, S. Leung, S. Longet, D. Ngabo, K.L. Osman, J. Paterson, E.J. Penn, S.T. Pullan, E. Rayner, O. Skinner, K. Steeds, I. Taylor, T. Tipton, S. Thomas, C. Turner, R.J. Watson, N.R. Wiblin, S. Charlton, B. Hallis, J.A. Hiscox, S. Funnell, M.J. Dennis, et al., Dose-dependent response to infection with SARS-CoV-2 in the ferret model and evidence of protective immunity, Nat. Commun. 12 (2021) 81.
[33] N. Osterrieder, L.D. Bertzbach, K. Dietert, A. Abdelgawad, D. Vladimirova, D. Kunec, D. Hoffmann, M. Beer, A.D. Gruber, J. Trimpert, Age-Dependent progression of SARS-CoV-2 infection in Syrian hamsters, Viruses 12 (2020) 779.
[34] C. Zhang, H. Cui, Z. Guo, Z. Chen, F. Yan, Y. Li, J. Liu, Y. Gao, C. Zhang, SARS-CoV-2 virus culture, genomic and subgenomic RNA load, and rapid antigen test in experimentally infected Syrian hamsters, J. Virol. 96 (2022) e0103422.
[35] M. Santos Bravo, C. Berengua, P. Marín, M. Esteban, C. Rodriguez, M. Del Cuerpo, E. Miró, G. Cuesta, M. Mosquera, S. Sánchez-Palomino, J. Vila, N. Rabella, M. Marcos, Viral culture confirmed SARS-CoV-2 subgenomic RNA value as a good surrogate marker of infectivity, J. Clin. Microbiol. 60 (2022) e0160921.